Journal of Molecular Catalysis B: Enzymatic 74 (2012) 144–150

Contents lists available at SciVerse ScienceDirect

Journal of Molecular Catalysis B: Enzymatic

journal homepage: www.elsevier.com/locate/molcatb

Kinetic resolution of glyceraldehyde using an aldehyde dehydrogenase from *Deinococcus geothermalis* DSM 11300 combined with electrochemical cofactor recycling

H. Wulf[a], M. Perzborn[a], G. Sievers[b], F. Scholz[b], U.T. Bornscheuer[a,*]

[a] Dept. of Biotechnology & Enzyme Catalysis, Institute of Biochemistry, Greifswald University, Felix-Hausdorff-Str 4, D-17487 Greifswald, Germany
[b] Dept. of Analytical & Environmental Chemistry, Institute of Biochemistry, Greifswald University, Felix-Hausdorff-Str 4, D-17487 Greifswald, Germany

ARTICLE INFO

Article history:
Received 28 March 2011
Received in revised form
11 September 2011
Accepted 17 September 2011
Available online 23 September 2011

Keywords:
Aldehyde dehydrogenase
Glyceraldehyde
Glyceric acid
Electrochemical cofactor regeneration
Kinetic resolution

ABSTRACT

Glyceraldehyde and glyceric acid are both valuable chiral starting materials. Aldehyde dehydrogenases (ALDHs) accept a broad scope of endo- and exogenous aldehydes, such as glyceraldehyde, and convert them into the corresponding carboxylic acid. Here we present cloning, overexpression and kinetic data on two ALDHs from *Escherichia coli* BL21 and *Deinococcus geothermalis*. The two ALDHs have a similar substrate scope and favor short to medium chain aldehydes, both oxidize glyceraldehyde to glyceric acid. The ALDH variant of *D. geothermalis* shows the higher specific activity towards glyceraldehyde and has an elevated activity optimum compared with the BL21 enzyme. The ALDH of *G. geothermalis* was also applied to conduct a kinetic resolution of glyceraldehyde with electrochemical cofactor recycling.

1. Introduction

Aldehyde dehydrogenases belong to an enzyme class widely spread over every kingdom of life, catalyzing the irreversible oxidation of a wide variety of endo- and exogenous aldehydes to their corresponding carboxylic acids. The protein YdcW of *Escherichia coli* has been described belonging to the superfamily of aldehyde dehydrogenases (ALDHs), and was annotated as betaine aldehyde dehydrogenase (EC 1.2.1.8). Kinetic studies revealed the enzyme should be more specifically described as medium chain aldehyde dehydrogenase (EC 1.2.1.3) [1,2]. Like many other ALDHs the crystal structure of the protein reveals a homotetrameric quarternary structure with a catalytic site and NAD^+ bound to each subunit. The subunits consist of a catalytic domain, a cofactor binding domain, and an arm-like oligomerisation domain including the C-terminus. The enzyme Dgeo_1120 represents an ALDH from the radiation resistant and thermophilic organism *Deinococcus geothermalis* (type strain DSM 11300) [3,4] and has been to the best of our knowledge not yet characterized. The enzyme was annotated as succinic-semialdehyde dehydrogenase.

The reaction mechanism of human ALDHs has been identified as an ordered sequential mechanism [5]. First, the NAD^+ cofactor binds to the enzyme. Secondly, an aldehyde is bound followed by a nucleophilic attack by the sulfur of a catalytic cysteine residue. The carbonyl hydride of the tetrahedral intermediate is then transferred to the C4 of the nicotinamide moiety of the NAD^+. The conformational change of the NADH then favors the activation of a water molecule by a glutamate residue. The water molecule attacks the substrate–enzyme thioester bond, and the corresponding carboxylic acid is released [5–7]. Studies on YdcW regarding conserved residues and NADH positioning, derived from crystal structures, suggest that a similar mechanism in bacterial ALDH can be assumed [2].

Glyceraldehyde (GLA) and glyceric acid (GA) are possible substrate and product of ALDH catalyzed reactions and both can serve as chiral building blocks. GLA for example can serve as structural motif in 4-(dihydroxyalkyl)-β-lactams [8,9]. GA is known as a liver stimulant in dogs and has effects on the acetaldehyde detoxification in rats [10,11]. GA is a building block in glycerate phospholipid analogues, e.g. acyl glycerate derivatives bearing an "inverse ester" function compared to natural phospholipids, at the carboxylic group of the GA that circumvents the hydrolysis by phospholipase PLA_1 [12].

The enzymes YdcW of *E. coli* BL21 (DE3) (ALDH-BL21) and dgeo_1120 of *D. geothermalis* 11300 (ALDH-11300) were cloned and examined during this work. Since ALDHs depend on expensive cofactors like NAD^+ or $NADP^+$ as electron acceptors, preparative scale biotransformations using these dehydrogenases require

* Corresponding author. Tel.: +49 3834 86 4367; fax: +49 3834 86 794367.
E-mail address: uwe.bornscheuer@uni-greifswald.de (U.T. Bornscheuer).

1381-1177/$ – see front matter © 2011 Elsevier B.V. All rights reserved.
doi:10.1016/j.molcatb.2011.09.011

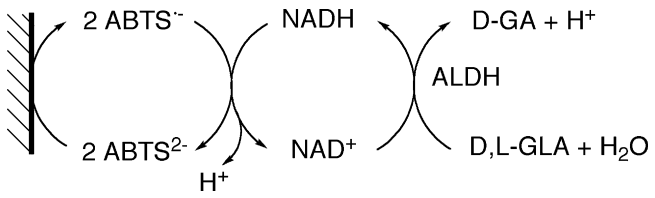

Fig. 1. Reaction scheme for the biocatalysis using ALDH and electrochemical cofactor recycling.

cofactor recycling systems like enzyme-coupled or substrate-coupled systems to reoxidize the cofactors [13]. In order to employ low concentrations of NAD^+ in the biotransformation of glyceraldehyde to glyceric acid, an electrochemical cofactor recycling system can be used. ALDHs in immobilized form have already been used in aldehyde oxidations with electrochemical cofactor regeneration [14]. Also glyceraldehyde was oxidized this way applying immobilized PQQ dependent oxidoreductases at modified glassy carbon electrodes [15]. NADH can be oxidized at carbon electrodes at neutral to alkaline pH but high overpotentials (above 1 V vs. Ag/AgCl) have to be applied [16,17]. The high positive potentials may lead to unspecific side products and enzyme deactivation. To circumvent the high potentials, NADH oxidation at glassy carbon could successfully be carried out using the 2,2-azinobis(3-ethylbenzothiazoline-6-sulfonate (ABTS) as mediator in a horse liver alcohol dehydrogenase based biotransformation approach [18].

In this paper we describe the cloning, overexpression and properties of two ALDHs such as kinetic data and oxidative kinetic resolution of glyceraldehyde (GLA) combined with electrochemical cofactor recycling using ALDH-11300 to yield glyceric acid (GA) (Fig. 1).

2. Experimental

2.1. Chemicals

All chemicals were purchased from Sigma–Aldrich (St. Louis, USA) and Carl-Roth (Karlsruhe, Germany). Polymerases were obtained from Roboklon (Berlin, Germany), Restrictions enzymes and DNA ligases were obtained from Fermentas (Burlington, Canada).

2.2. Bacterial strains, plasmids and growth conditions

E. coli BL21 (DE3) was purchased from Novagen (Darmstadt, Germany) and used as expression strain and for the isolation of genomic DNA. *D. geothermalis* DSM 11300 was obtained from DSMZ (Braunschweig, Germany). *E. coli* One Shot® TOP10 cells (F^- *mcr*A Δ(*mrr-hsd*RMS-*mcr*BC) Φ80*lac*ZΔM15 Δ*lac*X74 *rec*A1 *ara*D139 Δ(*araleu*)7697 *gal*U *gal*K *rps*L (Str^R) *end*A1 *nup*G) and vector pCR®II-TOPO® for subcloning were purchased from Invitrogen (Karlsruhe, Germany). *E. coli* strains were routinely cultured in lysogeny broth [19] without glucose at 37 °C, when necessary supplemented with ampicillin (100 μg/ml) or kanamycin (50 μg/ml). *D. geothermalis* was cultured in LB medium at 45 °C for four days. The expression plasmids pET-22b(+) and pET-28b(+) were obtained from Novagen (Darmstadt, Germany), the latter was used for enzyme expression with N-terminal His_6-tag.

2.3. Cloning of ydcW and aldh-11300

Genomic DNA (gDNA) from *E. coli* BL21 (DE3) and *D. geothermalis* was isolated using the innuPREP Bacteria DNA Kit (Analytik Jena, Jena, Germany). Plasmid isolations (Fermentas, Burlington, Canada), PCR-purification and gel extraction (Analytik Jena, Jena, Germany) were performed according to the manufacturer protocols. Standard procedures such as DNA cloning and manipulations were performed as described by Sambrook and Russell [20]. DNA sequencing was carried out by GATC Biotech AG (Konstanz, Germany).

The gene *ydcW* (*aldh*-BL21, GenBank accession code: GI:313848522, locus tag B21_01412, protein: YP_604587 (NCBI)) was amplified from gDNA of *E. coli* BL21(DE3) by PCR using the primer pair forward: 5′-CAT ATG CAA CAT AAG TTA CTG ATT AAC GGA G-3′ and reverse: 5′-GGA TCC TTA ATG TTT AAC CAT GAC GTG-3′. The gene *aldh*-11300 (GenBank accession code: GI:94554390, locus tag Dgeo_1120, protein: Q1IZB6_DEIGD (UniProt)) was amplified from gDNA of *D. geothermalis* DSM 11300 using the primer pair forward: 5′-CAT ATG ACC CCT GAC CCC CAG CAC CCT GAG AAG AC-3′ and reverse: 5′-GGA TCC TCA GCC CAC CAC CTG GGC AGC CTG GCC CCC GCT TCT GGA T-3′. PCR products were separated in a 1.2% agarose gel from which the desired fragments were purified, cloned into the vector pCR®II-TOPO® and *E. coli* One Shot® TOP10 cells were transformed with the plasmids bearing the respective insert. YdcW (ALDH-BL21) and ALDH-11300 in pCR®II-TOPO® were sequenced and cloned into pET-22b(+) and pET-28b(+) via NdeI and BamHI restrictions sites (underlined). Expression strain *E. coli* BL21 (DE3) was transformed with the four different originated vectors.

2.4. Expression of ALDH-BL21 and ALDH-11300 and enzyme purification

ALDH-BL21 and ALDH-11300, both with and without N-terminal His_6-tag, were expressed in *E. coli* BL21 (DE3) using 5 ml LB medium supplemented with 100 μg/ml ampicillin or 50 μg/ml kanamycin for expression control and activity measurements. Purified enzyme was obtained by the expression of His_6-tagged variants of the two enzymes in 500 ml LB medium containing 50 μg/ml kanamycin. Cells were grown at 37 °C to an optical density of 0.6 at 600 nm. Enzyme expression was induced with 0.4 mM IPTG and proceeded for 5–24 h at 30 °C. Cells were centrifuged (4000 × *g*, 4 °C, 15 min), the cell pellet was washed twice with 20 mM Tris–HCl buffer (pH 7.5) and disrupted in the same buffer by sonication (2–4 min, 30% power, 50% pulse). For biotransformation experiments cells were washed and resuspended with 50 mM sodium phosphate buffer (pH 7.5) (PB) and subsequently lysed in 50 mM sodium phosphate, 0.5 M NaCl (buffer A) using a French® Press (Thermo Fisher, Waltham, MA). The crude cell extract was centrifuged for 15 min at 16,000 × *g* and 4 °C and the supernatant was diluted 1:10 with buffer B (50 mM sodium phosphate, 0.5 M NaCl, 0.3 M imidazole, pH 7.5). For the purification of ALDH-BL21 and ALDH-11300 with the hexahistidine affinity tag (His_6-tag) the diluted crude extract was injected into a 5 ml HisTrap™ FF crude column for immobilized metal ion affinity chromatography (IMAC) using the ÄKTApurifer™ (GE-Healthcare, Munich, Germany). The column with bound enzyme was washed with 20% buffer B and fractions were collected while bound enzyme was eluted by applying 100% buffer B. For the storage of purified enzyme in solution or lyophilization, the purified enzyme was subjected to gel filtration for the removal of imidazole and high salt concentration using ÄKTApurifer™ equipped with Sephadex G-25 Superfine column (26 × 110 mm).

2.5. Determination of protein concentration and SDS-PAGE

Polyacrylamide gel electrophoresis was carried out using 4% stacking gel and 12% resolving gel according to the method described by Laemmli [21]. Roti-Mark® STANDARD (Roth, Karlsruhe, MW: 14–200 kDa) was used as protein standard. The

protein concentration was determined either with the BCA-assay (Uptima, Montluçon, France) or with Coomassie Brilliant-Blue using Roti®-Nanoquant (Carl-Roth, Karlsruhe, Germany) according to manufacturer protocols using BSA as standard.

2.6. Enzyme assays

The aldehyde dehydrogenase activity was determined spectrophotometrically at 30 °C by monitoring the rate of reduction of NAD^+ at 340 nm. The standard reaction mixture (1 ml) contained 80 mM Tris–HCl buffer (pH 9.0), 0.35 mM NAD^+, 2.5 mM D,L-glyceraldehyde and an appropriate amount of the enzyme. The reaction was started by adding D,L-glyceraldehyde to the mixture. One unit of aldehyde dehydrogenase activity was defined as the amount of enzyme that catalyzes the formation of 1 μmol NADH per minute.

In order to determine the apparent K_M and v_{max} values for different aldehydes the described activity test was carried out with varying substrate concentrations at a fixed concentration of 0.35 mM NAD^+. Initial velocities were recorded during the first 11 s of catalytic turnover. Apparent K_M and v_{max}-values were obtained by linear regression fitting of a Hanes plot. These values were used for non-linear regression, which effectively fits the data directly to the best hyperbola according to the method of Wilkinson [22] and Duggleby [23] using the program HYPER (J.S. Easterby, http://www.liv.ac.uk/~jse/software.html).

The effect of temperature on the enzyme activity was determined by incubating the standard reaction mixture at different temperatures ranging from 12 to 59 °C for 10 min at pH 9.0. For determining the effect of the pH towards enzyme activity, purified enzyme was incubated at 30 °C for 5 min in the following buffers at 100 mM: sodium acetate (pH 4.0–5.5), Bis–Tris–HCl (pH 5.5–7.0), sodium phosphate (pH 6.0–8.0) and Tris–HCl (pH 6.5–9.7) Activity was measured as described above.

2.7. Electrochemical measurements and biotransformations

Electrochemical measurements were carried out with an Autolab PSTAT 10 (Eco Chemie, Utrecht, Netherlands). All potentials refer to the Ag/AgCl electrode (3 mol l^{-1} KCl, $E = 0.208$ V vs. SHE). In cyclic voltammetry the second scan was used. The sweep rate was 5 mV s^{-1} and the potential range between 0 and 1 V vs. Ag/AgCl. The buffer system consisted of 100 mM sodium phosphate pH 8.0 (buffer PB).

Biotransformation experiments were carried out using the electrochemical cofactor recycling system. A foam glassy-carbon electrode (30 PPI RVC Duocel®, ERG Materials and Aerospace, Oakland, USA) was used as working electrode. A Pt-net surrounded the working electrode and served as auxiliary electrode. The above-mentioned Ag/AgCl reference electrode contacted the reactor via a KCl saturated agar tube (Fig. 2).

The buffer reaction solution consisted of 0.5 mM ABTS and 2 mM NADH in 20 ml of 100 mM sodium phosphate (pH 8.0). Experiments were performed at room temperature and the potential of the working electrode was hold at 0.7 V vs. Ag/AgCl. As biocatalyst a preparation of 5–10 U of purified and lyophilized ALDH-11300 was used. Racemic D,L-glyceraldehyde was added up to 40–50 mM.

2.8. Product determination by HPLC

Concentrations of glyceraldehyde (GLA) and glyceric acid (GA) were determined using a Shimadzu LC 10 HPLC equipped with a Eurokat-H precolumn (30 × 8 mm) and column (300 × 8 mm, both Knauer, Berlin, Germany) at 80 °C with 0.01 N sulfuric acid at 0.8 ml/min flow rate and refractive index detection. Chiral analysis of glyceric acid was conducted using a Merck Hitachi LaChrom HPLC equipped with a Chiralpak® QN-AX precolumn (4 × 10 mm) and column (4.6 × 150 mm, both Chiral Technologies Europe, Illkirch, France) at 23 °C with methanol/acetic acid/ammonia acetate 98/2/0.5 (v/v/w) as eluent at 1 ml/min flow rate and evaporative light scattering detection. The retention time of L-GA was 5.9 min and the D-GA retention time was 7.1 min.

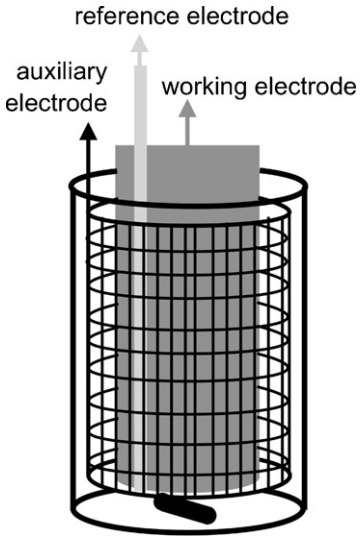

Fig. 2. Scheme of the biotransformation reactor vessel. The carbon foam working electrode is cylindrically surrounded by a platinum net shaped auxiliary electrode. The Ag/AgCl reference electrode is contacted via a KCl solution saturated agar tube. The electrodes are located inside a stirred 100 ml beaker.

3. Results and discussion

3.1. Amplification, cloning and protein expression of ALDH-BL21 and ALDH-11300

The genes encoding proteins ALDH-BL21 and ALDH-11300 could be successfully amplified and cloned into pET-22b(+) without His_6-tag and pET-28b(+) bearing the genes with N-terminal His_6-tag in order to enhance and simplify the protein purification procedure. The cloned DNA sequence of the *ydcW* differed in one nucleotide (A994G) to the database entry B21_01412. This difference leads to the mutation S332G at protein level in ALDH-BL21. Both genes could be overexpressed in the host strain *E. coli* BL21 (DE3). The His_6-tag variants of ALDH-BL21 and ALDH-11300 were purified to apparent homogeneity by IMAC (as determined by SDS-PAGE, data not shown) at yields of 39% (ALDH-BL21) and 66% (ALDH-11300) of the total activity.

3.2. Temperature- and pH-optimum

Since both enzymes could be expressed in active form with and without His_6-tag, subsequent experiments were performed with the His_6-tagged enzyme variants using glyceraldehyde as substrate. The temperature optimum of ALDH-BL21 from *E. coli* was between 30 and 35 °C (Fig. 3). The maximum activity for the ALDH-11300 from the mesothermophilic organism *D. geothermalis* was determined to be more than 10 °C higher, between 43 and 47 °C (Fig. 3), making this enzyme more useful for applications at elevated temperatures around 45 °C. The temperature range corresponds to the optimum growth temperature of *D. geothermalis* of 45–50 °C [3] since chaperones and compatible solutes may additionally stabilize the enzyme at temperatures of over 45 °C in its physiological environment.

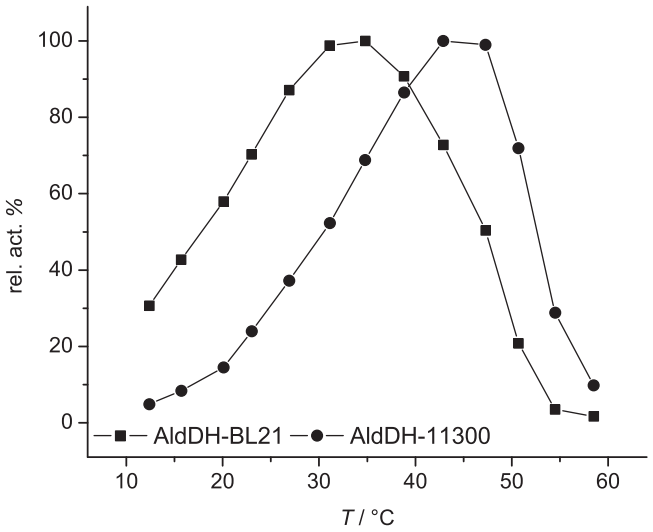

Fig. 3. Temperature profiles of ALDH-BL21 (■) and ALDH-11300 (●).

Both enzymes showed the highest activity at pH 8.5 in Tris–HCl. At pH 5.5 the enzymes showed residual activities of 10% and a complete loss of activity took place at pH 4.0 (Fig. 4).

3.3. Activity and steady-state kinetics

For ALDH-11300 from *D. geothermalis*, the oxidation of glyceraldehyde and other substrates was measured for the first time in this work. For the homolog ALDH enzyme from *E. coli* K12 activity against glyceraldehyde was previously described by Gruez et al. [2]. Activity could also be confirmed here for ALDH-BL21 from *E. coli* BL21, which differs in one amino acid (V197I) from the K12 variant. For this enzyme a specific activity of 0.6 U/mg was determined after IMAC purification. The newly characterized ALDH-11300 with a specific activity of 3.5 U/mg is more active against glyceraldehyde compared to ALDH-BL21. The purified ALDH-BL21 had only 2% activity against GLA with $NADP^+$ compared to NAD^+ as cofactor. ALDH-11300 showed 15% activity against GLA using $NADP^+$ instead of NAD^+. Gruetz et al. found 6% activity using $NADP^+$ in GLA oxidation, whereas the v_{max}/K_M ratio for $NADP^+$ is still 25% of the NAD^+ value [2].

The biocatalytic reduction of GLA and GA with NADH was investigated too. However no activity was observed with both enzymes towards GLA or GA. Eriksson et al. [10] showed that treatment of rats with GA enhances ethanol and acetaldehyde clearance. The authors suggest that GA enhances acetaldehyde detoxification by enhanced cofactor regeneration through ALDH catalyzed substrate reductions. Since the BRENDA-Database [24] solely lists one example of a ALDH converting an acid to an aldehyde, namely 3-hydroxypropionic acid to 3-hydroxypropionaldehyde with a poor activity of 4% of the oxidation capacity [25] and data of this work show no action of ALDH against glyceric acid this hypothesis seems to be unlikely. Because of the high difference in the redox potential, acids need to be phosphorylated prior to be metabolized and reduced by aldehyde dehydrogenases at reasonable reaction velocities.

Both aldehyde dehydrogenases showed no activity towards 1-propanol, 1,2-propandiol and glycerol as substrates. These findings indicate the chemoselectivity of these enzymes towards the oxidation of a terminal carbonyl group.

The activity of ALDH-11300 against several substrates was determined, and the kinetic parameters of the Michaelis–Menten equation were determined for six substrates at various concentrations (Table 1). The highest turnover rates were found for the oxidation of isobutyraldehyde. The slowest turnover was observed with the aromatic substrate phenylacetaldehyde. However with 3.76 s^{-1} mM^{-1} the k_{cat}/K_M value was still better than that of glyceraldehyde, which had the second best turnover but also the second highest K_M. The best k_{cat}/K_M was determined for butyraldehyde. Since no constants could be determined for valeraldehyde (C5) and caproaldehyde (C6), butyraldehyde represents the best kinetic data for the longest unbranched carbon chain. Valeraldehyde showed a significant inactivation above 150 μM (Fig. 5). The plots for caproaldehyde and valeraldehyde showed a non Michaelis–Menten like, sigmoidal slope.

Kinetic data were also determined for the ALDH-BL21. Similar to the findings of Gruez et al. our data show an increase in the turnover as the chain length of the substrate increases. In contrast to the findings for the K12-ALDH [2], the best substrate according to v_{max} values is the C4 substrate butyraldehyde. The best k_{cat}/K_M value has isobutyraldehyde before caproaldehyde (Table 2).

The enzyme activity after storing at 0 °C and at room temperature (RT) was determined during more than 40 days. ALDH-BL21 was more stable than ALD-11300 during both storing conditions. Activity of ALDH-BL21 after storing at 0 °C for 20 days showed 95%

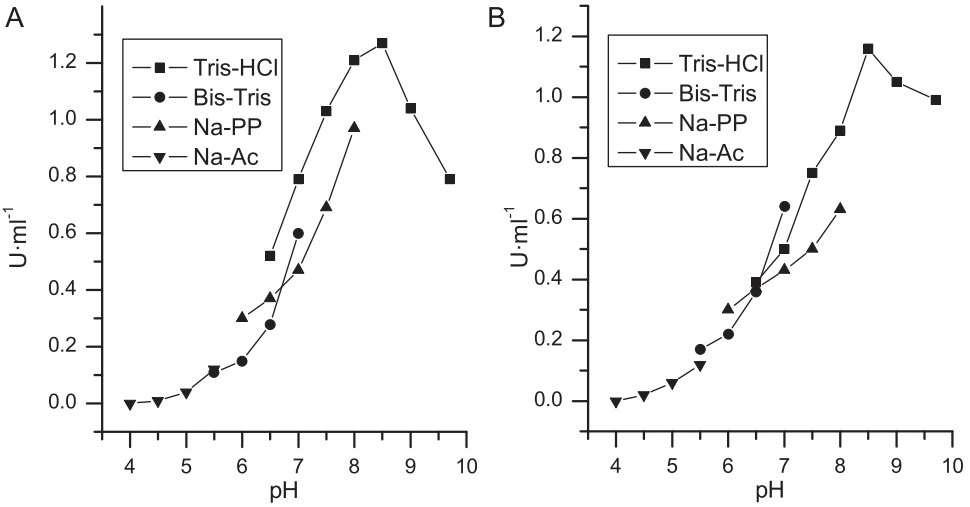

Fig. 4. Effect of pH on the enzyme activity in the range from pH 4.0 to 9.7 with for different buffers: sodium acetate (▼) Bis–Tris–HCl (●), sodium phosphate (▲) und Tris–HCl (■). (A) Activity of ALDH-BL21. (B) Activity of ALDH-11300.

Table 1
Kinetic parameters of ALDH-11300 for six substrates, ordered according to increasing k_{cat}-values. The error estimations represent a confidence interval of 95%.

Substrate	v_{max} [U mg^{-1}]	K_M [mM]	k_{cat} [1 s^{-1}]	k_{cat}/K_M [1 s^{-1} mM^{-1}]
Phenylacetaldehyde	1.74 ± 0.24	0.13 ± 0.07	1.56 ± 0.22	12.4 ± 3.35
Acetaldehyde	1.97 ± 0.14	0.21 ± 0.06	1.78 ± 0.13	8.59 ± 2.06
Propionaldehyde	2.76 ± 0.16	0.14 ± 0.03	2.49 ± 0.14	17.39 ± 4.65
Butyraldehyde	2.9 ± 0.4	0.07 ± 0.04	2.61 ± 0.36	37.74 ± 9.9
Glyceraldehyde	3.05 ± 0.35	2.52 ± 0.95	2.75 ± 0.32	1.09 ± 0.33
Isobutyraldehyde	3.22 ± 0.15	2.67 ± 0.4	2.9 ± 0.13	1.09 ± 0.33

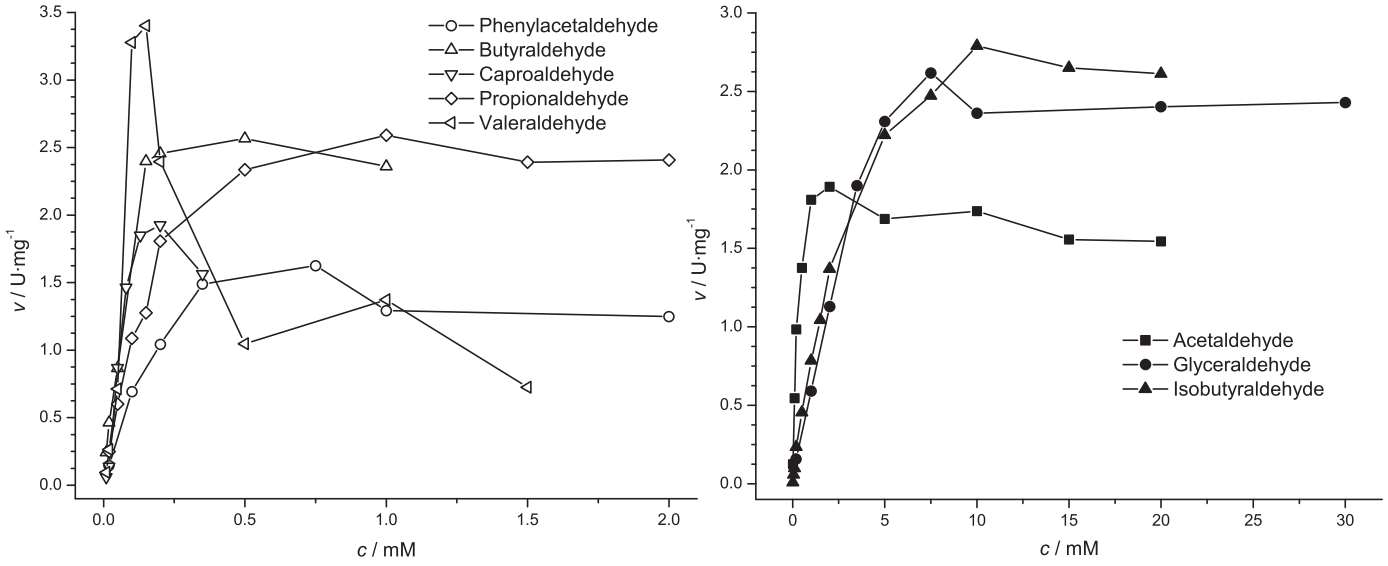

Fig. 5. The activity of ALDH-11300 towards several substrates at different concentrations.

Table 2
Kinetic parameters of ALDH-BL21 for eight substrates, ordered according to increasing k_{cat}-values. The error estimations represent a confidence interval of 95%.

Substrate	v_{max} [U mg^{-1}]	K_M [mM]	k_{cat} [1 s^{-1}]	k_{cat}/K_M [1 s^{-1} mM^{-1}]
Phenylacetaldehyde	0.08 ± 0.03	4.87 ± 3.98	0.07 ± 0.03	0.01 ± 0.01
Acetaldehyde	0.42 ± 0.01	0.56 ± 0.06	0.38 ± 0.01	0.67 ± 0.14
Isobutyraldehyde	0.55 ± 0.03	0.02 ± 0.004	0.49 ± 0.03	26.47 ± 5.94
Glyceraldehyde	0.95 ± 0.1	8.44 ± 2.66	0.86 ± 0.09	0.1 ± 0.03
Propionaldehyde	1.08 ± 0.04	0.05 ± 0.01	0.97 ± 0.04	21.05 ± 4.21
Valeraldehyde	1.24 ± 0.11	0.07 ± 0.02	1.12 ± 0.1	16.28 ± 4.73
Caproaldehyde	1.41 ± 0.11	0.05 ± 0.02	1.27 ± 0.1	25.21 ± 6.04
Butyraldehyde	1.64 ± 0.25	0.08 ± 0.04	1.48 ± 0.23	18.98 ± 5.8

of the initial value, whereas for ALD-11300 activity was reduced by 40% (0 °C) to 80% (room temperature) (Fig. 6). Storage of purified enzymes at −20 °C resulted in complete loss of activity, but freeze dried ALDH-11300 retained 80% of its activity towards GLA.

3.4. Biotransformation and determination of reaction products

Glyceraldehyde should be oxidized to GA in an ALDH catalyzed kinetic resolution. For these biotransformation experiments 100 mM sodium phosphate pH 8.0 was used instead of Tris-buffer, because tris (tris(hydroxymethyl)-aminomethane) is not applicable in reactions with acyl-enzyme intermediates since it may act as nucleophile itself [26]. Cyclic voltammetry measurements show the two-electron transfer system of ABTS. The first redox reaction is reversible and important for the NADH reoxidation. The second (more positive) redox system is irreversible and must be avoided as otherwise ABTS is eliminated from the equilibrium. The cyclic voltammogram of NADH shows an irreversible system with a current peak at 580 mV vs. Ag/AgCl (Fig. 7, plot d). A solution of 4 mM NADH and 1 mM ABTS shows an irreversible oxidation peak at 500 mV since ABTS$^{\bullet-}$ is immediately

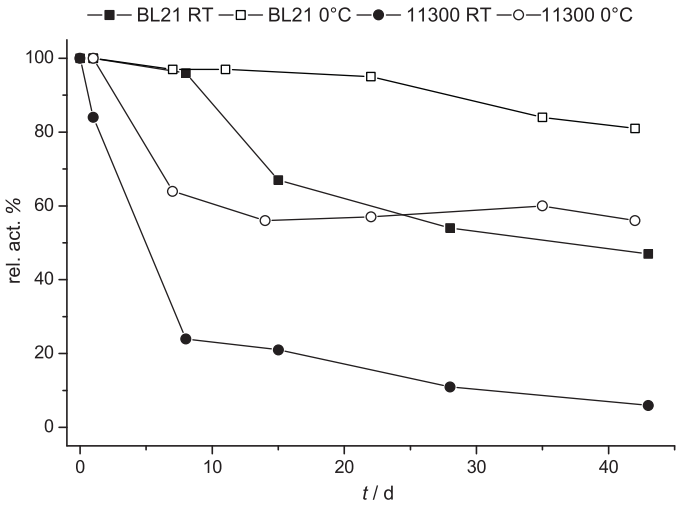

Fig. 6. Activity of the enzymes ALDH-BL21 und ALDH-11300 after storing at room temperature and at 0 °C for 43 days.

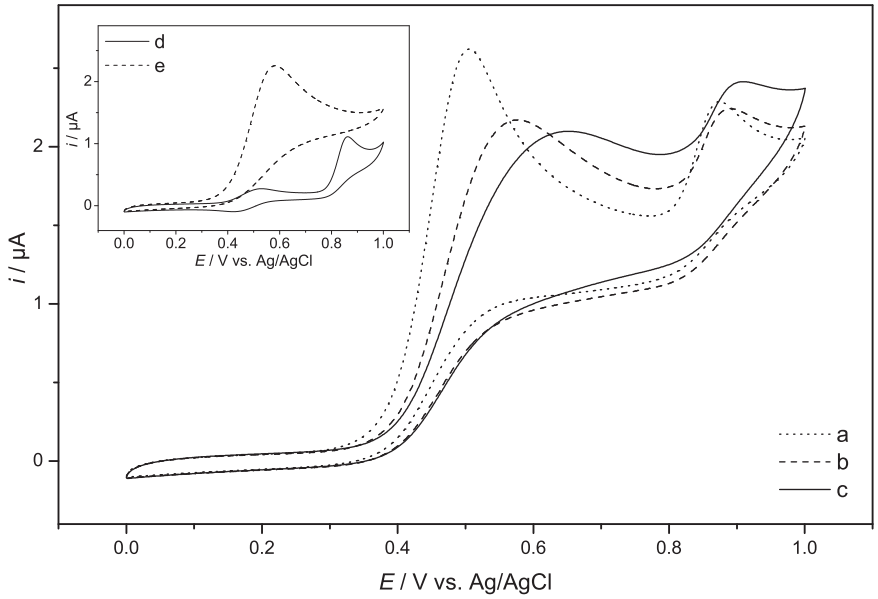

Fig. 7. The plot a displays the CV of ABTS and NAD, b displays ABTS, NAD and ALDH-11300, c displays ABTS, NAD, ALDH-11300 and GLA, d displays NAD (4 mM) and e displays ABTS (1 mM). All CVs were measured in PB (100 mM, pH 8.0).

oxidized by NADH (Fig. 7 and [18]). The addition of enzyme and GA shifts the current peak of the recycling system to higher overpotentials, which may be due to blocking of catalytic active sites at the electrode. The increase of the overpotential of the recycling system requires a higher potential as it would be needed for normal ABTS mediated NADH reoxidation. The potential for the biotransformation should be at least 650 mV vs. Ag/AgCl (Fig. 7) thus for biotransformation experiments 700 mV where applied.

During the biotransformation experiments, the cofactor NADH was indirectly recycled at constant potential of 700 mV at a glassy carbon foam electrode. The foam electrode was used to generate a greater contact surface, where ABTS and subsequently NADH could be reoxidized (Fig. 1). The reaction vessel contained 20 ml buffer solution with dissolved enzyme and substrates. Since NADH was applied initially, the reaction started only after the current was switched on. Samples were taken during the biocatalysis and analyzed via ion-exclusion and chiral HPLC, and the transferred electric charge was monitored (Fig. 8). In biotransformation A the concentration of GA increased by 16.4 mM while the concentration of GLA decreased by 14.5 mM (Fig. 8). Biotransformation B does not show such a high accumulation of D-GA, it increases by 7.9 mM while GLA drops in 12.7 mM (Fig. 8). The small experimental discrepancies between drop of educts and gain of products are most probably experimental errors. The measured transferred charge (q_m) apparently fits the theoretically transferred charge (q_t) best in the beginning of the biocatalysis (Fig. 8). The difference between q_m and q_t gains significance with progression of the reaction. A subsequent oxidation of glyceric acid at the anode is not possible, as proven in separate CV experiments (data not shown), hence further oxidation of GA is not an explanation for the differing q_t and q_m. A possible explanation could be the big surface and the large number of pores and cavities of the carbon foam electrode. GLA and GA may diffuse into the pores, and hence evade the chromatographic quantitation. Washing steps of the working electrode after the biotransformation revealed that GA and GLA where retained by the electrode and perhaps remained in the cavities. This can lead to a systematic error in the determination of the extent of the biotransformation. The structure of

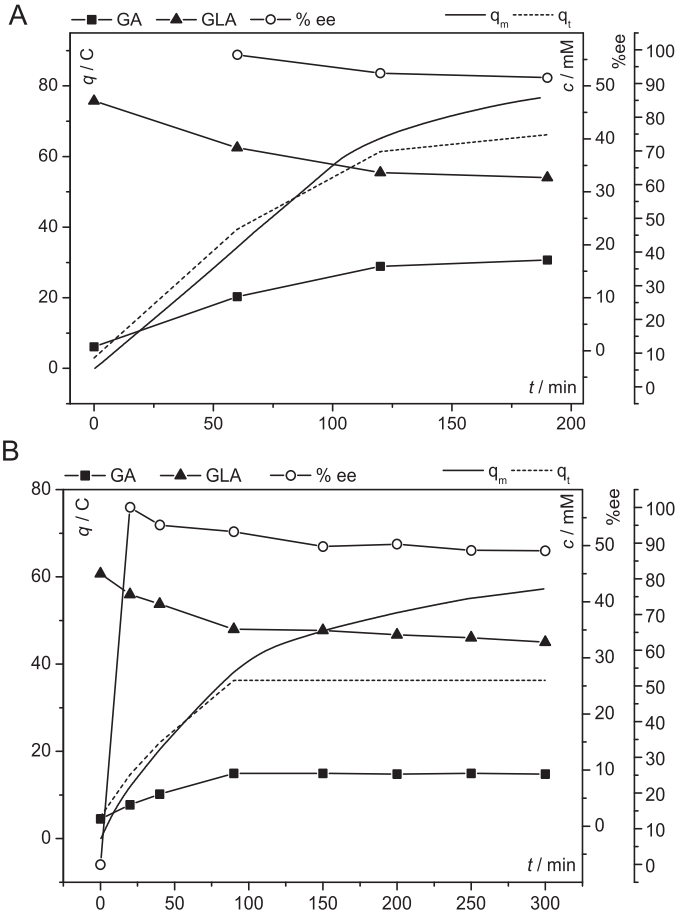

Fig. 8. Plots of biotransformation experiments A and B. The reactions differ solely in the prolonged reaction time and greater number of sample points in biotransformation B. q_m and q_t refer to the left axis, concentrations of GLA, GA and *%ee* to the two left axes.

the porous working electrode will certainly lead to lower potentials inside the pores, which will decrease the electrolysis efficiency [27]. This feature must receive further attention when an upscaling of the technique is intended. It might also be possible that with reaction time the enzyme becomes oxidized at the electrode as described by Manjón et al. for glucose dehydrogenase [28], which can be an explanation for the uncompleted conversion of the GLA.

The enantiomeric excess of the resulting D-GA decreased during both biotransformations although no direct oxidation of GLA at the electrode could be observed at the applied potential. At the first measurement, the enantiomeric excess of both reactions was still 98.5%*ee* and 100%*ee* but ended up in 91.8 and 87.9%*ee*, respectively (Fig. 8).

4. Conclusion

In this work we showed the cloning, purification, characterization and biocatalysis with two ALDH from *E. coli* BL21 and *D. geothermalis*. Both enzymes could be overexpressed and purified with IMAC yielding 39–66% active enzyme. The ALDH-11300 with 3.5 U/mg had a better specific activity against glyceraldehyde then ALDH-BL21 with 0.6 U/mg. The pH profile was similar for both enzymes and showed the highest activity at a pH of 8.5. The temperature optimum of activity at 45–50 °C was 10 °C higher with ALDH-11300 then with ALDH-BL21. The best substrate according to k_{cat}/K_M for ALDH-11300 and ALDH-BL21 were butyraldehyde and isobutyraldehyde, respectively. Biotransformations of GLA to GA with ALDH-11300 and electrochemical cofactor recycling led to concentrations up to 1.8 g/l D-GA with 88%*ee*.

Acknowledgements

The authors thank the “Fachagentur für Nachwachsende Rohstoffe” (AZ06NR073, 22015906) for financial support.

References

[1] N.A. Sophos, V. Vasiliou, Chem. Biol. Interact. 143–144 (2003) 5–22.
[2] A. Gruez, V. Roig-Zamboni, S. Grisel, A. Salomoni, C. Valencia, V. Campanacci, M. Tegoni, C. Cambillau, J. Mol. Biol. 343 (2004) 29–41.
[3] A.C. Ferreira, M.F. Nobre, F.A. Rainey, M.T. Silva, R. Wait, J. Burghardt, A.P. Chung, M.S. Da Costa, Int. J. Syst. Bacteriol. 47 (1997) 939–947.
[4] K.S. Makarova, M.V. Omelchenko, E.K. Gaidamakova, V.Y. Matrosova, A. Vasilenko, M. Zhai, A. Lapidus, A. Copeland, E. Kim, M. Land, K. Mavromatis, S. Pitluck, P.M. Richardson, C. Detter, T. Brettin, E. Saunders, B. Lai, B. Ravel, K.M. Kemner, Y.I. Wolf, A. Sorokin, A.V. Gerasimova, M.S. Gelfand, J.K. Fredrickson, E.V. Koonin, M.J. Daly, PLoS ONE 2 (2007) e955.
[5] R.I. Feldman, H. Weiner, J. Biol. Chem. 247 (1972) 267–272.
[6] P.K. Hammen, A. Allali-Hassani, K. Hallenga, T.D. Hurley, H. Weiner, Biochemistry 41 (2002) 7156–7168.
[7] S.J. Perez-Miller, T.D. Hurley, Biochemistry 42 (2003) 7100–7109.
[8] D.R. Wagle, C. Garai, J. Chiang, M.G. Monteleone, B.E. Kurys, T.W. Strohmeyer, V.R. Hegde, M.S. Manhas, A.K. Bose, J. Org. Chem. 53 (1988) 4227–4236.
[9] P. Areces, E. Carrasco, M.E. Light, M. Santos, J. Plumet, Synlett 2007 (2007) 3180–3182.
[10] C.J.P. Eriksson, T.P.S. Saarenmaa, I.L. Bykov, P.U. Heino, Metabolism 56 (2007) 895–898.
[11] S.S. Handa, A. Sharma, K.K. Chakraborti, Fitoterapia 57 (1986) 307.
[12] R. Rosseto, C.M. Tcacenco, R. Ranganathan, J. Hajdu, Tetrahedron Lett. 49 (2008) 3500–3503.
[13] W. Kroutil, H. Mang, K. Edegger, K. Faber, Curr. Opin. Chem. Biol. 8 (2004) 120–126.
[14] C.M. Moore, N.L. Akers, A.D. Hill, Z.C. Johnson, S.D. Minteer, Biomacromolecules 5 (2004) 1241–1247.
[15] R.L. Arechederra, S.D. Minteer, Electrochim. Acta 55 (2010) 7679–7682.
[16] S.B. Saidman, J.B. Bessone, Electrochim. Acta 45 (2000) 3151–3156.
[17] C. Kohlmann, W. Märkle, S. Lütz, J. Mol. Catal. B: Enzym. 51 (2008) 57–72.
[18] I. Schröder, E. Steckhan, A. Liese, J. Electroanal. Chem. 541 (2003) 109–115.
[19] G. Bertani, J. Bacteriol. 62 (1951) 293–300.
[20] J. Sambrook, D.W. Russell, Molecular Cloning: A Laboratory Manual, 3rd ed., Cold Spring Harbor Laboratory Press, New York, 2001.
[21] U.K. Laemmli, Nature 227 (1970) 680–685.
[22] G.N. Wilkinson, Biochem. J. 80 (1961) 324–332.
[23] R.G. Duggleby, Anal. Biochem. 110 (1981) 9–18.
[24] M. Scheer, A. Grote, A. Chang, I. Schomburg, C. Munaretto, M. Rother, C. Söhngen, M. Stelzer, J. Thiele, D. Schomburg, Nucl. Acids Res. 39 (2010) 1–7.
[25] J.-E. Jo, S. Mohan Raj, C. Rathnasingh, E. Selvakumar, W.-C. Jung, S. Park, Appl. Microbiol. Biotechnol. 81 (2008) 51–60.
[26] V. Kasche, R. Zöllner, Hoppe Seylers Z. Physiol. Chem. 363 (1982) 531–534.
[27] R.E. Sioda, Electrochim. Acta 16 (1971) 1569–1576.
[28] A. Manjón, J.M. Obón, P. Casanova, V.M. Fernández, J.L. Ilborra, Biotechnol. Lett. 24 (2002) 1227–1232.